2023 IEEE Wireless and Microwave Technology Conference (WAMICON) | 979-8-3503-9864-9/23/$31.00 ©2023 IEEE | DOI: 10.1109/WAMICON57636.2023.10124924

Co-Design of Doherty Power Amplifier and Post-Matching Bandpass Filter

Haifeng Lyu
Electrical and Computer Engineering
University of Central Florida
Orlando, USA
Haifeng@Knights.ucf.edu

Ricardo Lovato
Applied Physics Lab
Johns Hopkins University
Laurel, USA
RLovato@Knights.ucf.edu

Shakthi Priya Gowri
Electrical and Computer Engineering
University of Central Florida
Orlando, USA
ShakthiPriyaGowri@Knights.ucf.edu

Xun Gong
Electrical and Computer Engineering
University of Central Florida
Orlando, USA
Xun.Gong@ucf.edu

Kenle Chen
Electrical and Computer Engineering
University of Central Florida
Orlando, USA
Kenle.Chen@ucf.edu

***Abstract*—This paper presents a novel co-designed Doherty power amplifier (DPA) and a post-matching output bandpass filter. The filter is designed as a matching network to present the desired impedance at the combining node of carrier and peaking paths, thus eliminating the quarter-wave transformer of the conventional Doherty combiner network. This co-design method minimizes the circuit complexity and inter-connection loss, leading to an enhanced overall performance. A prototype is designed and implemented using GaN transistors and third-order Hairpin filter with 20% bandwidth centered at 3.6 GHz. The measured frequency response exhibits desired amplifier-filter function, and Doherty efficiency enhancement are experimentally demonstrated with efficiency of 68% and 55% at saturation and 6-dB back-off regions. Modulated measurement shows excellent linearity (37-dB adjacent channel leakage ratio) and efficiency (47%) for transmitting the LTE signal with 10.5-dB PAPR.**

***Index Terms*—Co-design, Doherty, filter, high efficiency, load modulation, matching, power amplifier.**

I. Introduction

In a typical wireless radio frontend, the power amplifier (PA) is normally followed by a bandpass filter, which is shared with the receive path in a time-domain duplex system. For the transmit mode, the filter offers post frequency selection, harmonic rejection, and spectral emission regulation. Conventionally, the PA and filter are designed independently based on 50-Ω system impedance as the connection interface. However, this method does not engender the best possible performance, since no global optimization along the transmitter chain is achieved.

Recently, co-design and direct integration of PA and filter have been extensively studied [1]–[3]. By merging the PA output matching into the filter design, it offers minimized form factor, reduced interconnection loss, and enhanced performance. It is important to note that the reported works are mostly focused on single-branch PAs, such as Class-F [4], Class-J [1], continuous Class-F [5], etc. However, the use of complex modulation schemes, i.e., high-order quadrature amplitude modulation (QAM) and orthogonal frequency domain multiplexing (OFDM), in the latest wireless standards have led to the significant increase of signals' peak to average power ratio (PAPR) and degradation of PA efficiency. The Doherty PA (DPA) emerges as an effective solution for efficient amplification of high-PAPR signals, and it has been massively adopted in the cellular base stations. In [6], the filter is co-designed with the input quadrature divider of a DPA.

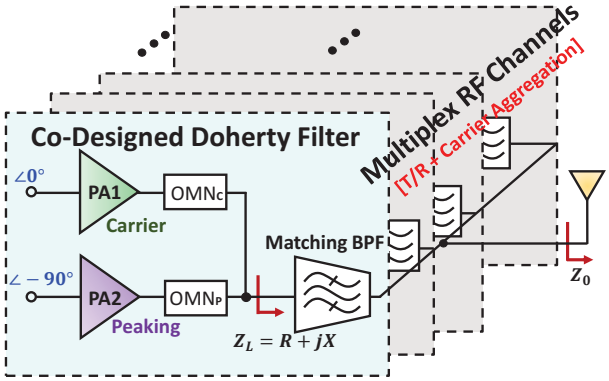

Fig. 1. Concept of co-designed DPA and post-select bandpass filter.

This paper investigates, for the first time, the concept of co-designed of Doherty PA and a post-matching output bandpass filter. As illustrated in Fig. 1, the bandpass filter can be designed as a post-matching network to transform the antenna impedance Z_0 to the optimal Doherty combining load Z_L to replace the traditional quarter-wave transmission line (T-line) and merge the sectorized PA-filter module. This integrated Doherty filter architecture can operate at specific bands and directly inherit the benefits of co-design in terms of size, loss, and performance. The proposed concept is experimentally validated with a physical prototype implemented using a GaN-based DPA and a third-order Hairpin matching filter, which exhibits state-of-the-art linearity and efficiency.

II. Co-Design of Doherty PA and Bandpass Filter

The Doherty topology is constructed with carrier and peaking amplifiers biased in Class-AB and Class-C modes to improve the back-off efficiency. These two PAs are combined to a common load Z_L and then transformed to the load termination Z_0 through a quarter-wave T-line. Conventionally, a real impedance $Z_0/2$ is presented to the common load to provide $2Z_0$ to the carrier amplifier at the low-power region (peaking off). Recently, the post matching technique has been proposed [7]–[9] to provide fundamental load termination, in which the quarter-wave transformer is replaced by a matching network post to the combining node. This post matching circuit can covert the antenna impedance Z_0 to a complex common load Z_L, thus largely increases the design freedom for wideband and linear DPA.

In this paper, we go one step further and show that this post matching network can also be integrated into output matching filter as presented in Fig. 2(a), which is targeted for the realistic radio front-end with frequency selectivity and impedance transformation. Moreover, the Z_0-T-line combiner can be absorbed into the matching network of carrier side amplifier, so that both OMNs of carrier and peaking can be equivalent to an ideal transformer in series with a T-line with certain phase offset as shown in Fig. 2(b). Therefore, during load modulation, the $Z_{\rm C}$ ($Z_{\rm P}$) at current source plane can be derived through the ABCD matrix analysis of OMNc and OMNp,

$$Z_{\rm C/P} = \frac{Z'_{\rm C/P}\cos\theta_{\rm C/P} + jZ_0\sin\theta_{\rm C/P}}{Z'_{\rm C/P}j(\sin\theta_{\rm C/P})/Z_0 + \cos\theta_{\rm C/P}} \tag{1}$$

where the $Z'_{\rm C}$ ($Z'_{\rm P}$) represents the impedance seen towards combining node at carrier (peaking) path. When the peaking device is turned off at power back off, the carrier impedance can be expressed as

$$Z_{\rm C\_OBO} = \frac{Z_{\rm L} \times Z'_{\rm P\_OBO}}{Z_{\rm L} + Z'_{\rm P\_OBO}} \tag{2}$$

in which $Z'_{\rm P\_OBO}$ can be easily obtained with $Z_{\rm P\_OBO} = \infty$. Once the common load Z_L is determined, the impedance at source plane can be calculated from Eqs. (1) and (2) and vice versa. It is worthy to note that the OMN of carrier and peaking amplifiers can also be merged into the output filter combining network, leading to a fully co-designed Doherty filter module and minimized complexity of PA matching.

As the key enabler to this technology, the matching filter can be represented by the coupling matrix. To transform the load Z_0 to $Z_{\rm L}$, the original coupling matrix of the filter can be synthesized as indicated in Fig. 2(a) assuming a third-order Chebyshev bandpass filter [2]. In this letter, the common load $Z_{\rm L}$ is properly designed to a resistive impedance at target frequency. Therefore, only the source coupling coefficient ($M_{4\rm L}$) needs to be modified and the external couplings ($Q_{\rm ext}$) for source and load are physically asymmetric as indicated by the $Z_{\rm L}$ expression in Fig. 2(a).

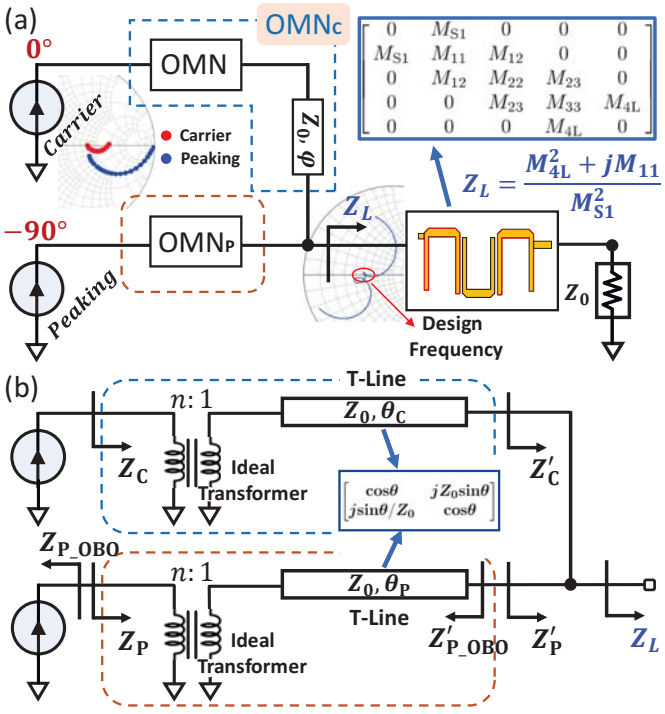

Fig. 2. Co-design of GaN Doherty PA and post-matching Hairpin filter.

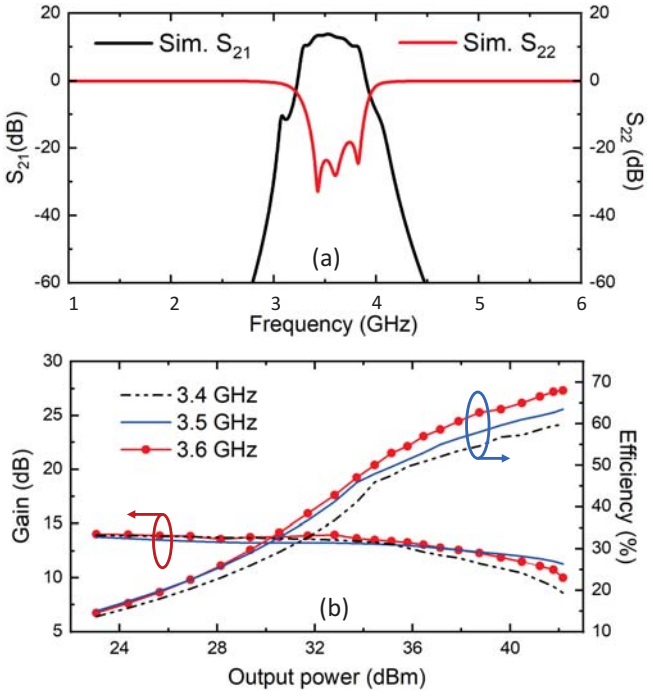

Fig. 3. Simulation results: (a) small-signal frequency responses of transmission and output reflection, (b) in-band power-swept DPA performance.

III. Physical Prototype Design

Based on the filter-post-matching technique, a prototype Doherty-filter is designed using GaN transistors (WolfSpeed CGH40006) and a third-order Hairpin filter. In this prototype, the carrier and peaking are symmetrically sized, and DPA architecture is illustrated in Fig. 2(a). The degrees of freedom

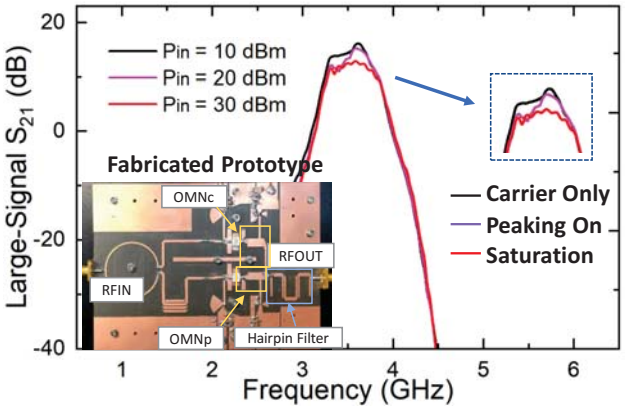

Fig. 4. Large-signal frequency response and the fabricated prototype demo of the co-designed DPA.

in this DPA design primarily involve $Z'_{\rm C}$, $Z'_{\rm P}$, n, $\theta_{\rm c}$, $\theta_{\rm p}$, and Z_L, while this target of this design is on not only the enhanced back-off efficiency but also high linearity. Moreover, proper harmonic loading is designed for both carrier and peaking amplifiers to perfect the efficiency and linearity followed [10]. After optimization using Keysight Advanced Design System (ADS), the combining load $Z_{\rm L}$ is selected around $25 - 1.5j$ Ω, and $Z'_{\rm C}$ and $Z'_{\rm P}$ are matched to around 50 Ω.

The load modulation behaviors (left inset Smith Chart of Fig. 2(a)) of two sub-amplifiers are controlled through phase alignment between two paths, i.e., $\theta_{\rm c}$ and $\theta_{\rm p}$, which are globally optimized with output matching networks and the phase offset line (Z_0, ϕ). The Hairpin filter is designed with a 20% fractional bandwidth centered at 3.6 GHz and an insertion loss of 0.5 dB. It transforms the 50Ω load to a $Z_{\rm L}$ matching impedance at the combining node, as depicted in the right Smith Chart of Fig. 2(a). The simulated small-signal frequency response of the designed Doherty filter is shown in Fig. 3(a), and the corresponding in-band large-signal simulation results are shown in Fig. 3(b). Desired filter-amplifier response and Doherty-type of back-off efficiency enhancement are clearly observed.

TABLE I
COMPARISON OF GAN PAS WITH INTEGRATED FILTERS

Ref.	f_0 (GHz)	Gain † (dB)	DE@$P_{\rm Max}$ (%)	DE@OBO (%)	$P_{\rm out}$ (dBm)
[1]	3	10.0	67	36*	41
[3]	4.7	13.7	55 (PAE)	37	37
[5]	1.8	12.3	74.5	34	40.3
[7]	2	14.1	74	39	38.9
[11]	3.5	12.6	68	38	40
[12]	2.4	18.2	71	39	41
T. W.	3.6	12.5	68	55	42

† Large-signal, * Graphically estimated.

IV. IMPLEMENTATION AND EXPERIMENTAL RESULTS

The co-designed Doherty-filter module is implemented on a 20-mil thick Rogers Duroid-5880 PCB board, as shown in the inset of Fig. 4. The carrier and peaking amplifiers are biased

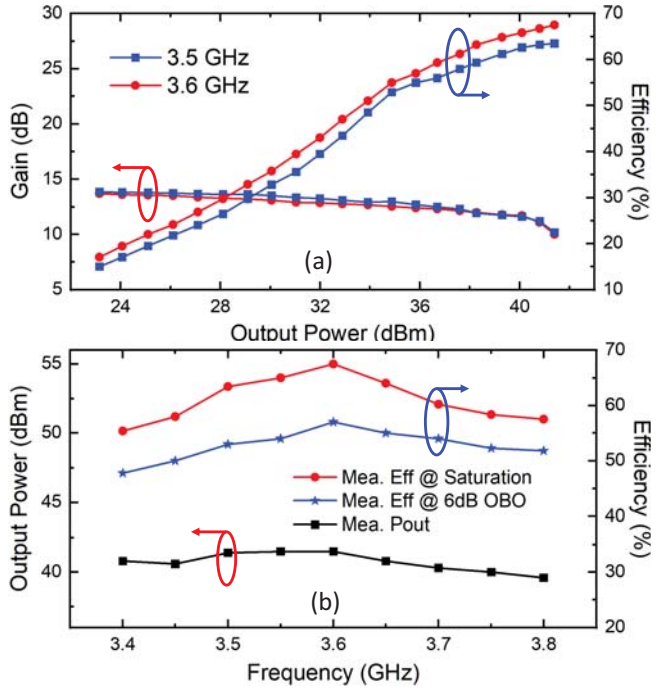

Fig. 5. CW measurement: (a) efficiency and gain versus output power at 3.5 and 3.6 GHz, (b) PA performance versus frequency across the pass-band.

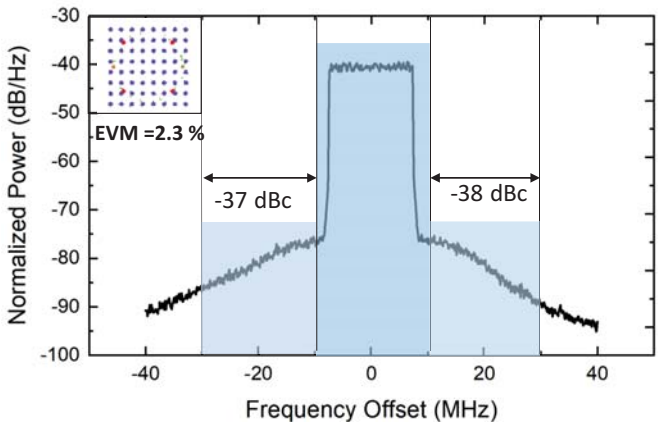

Fig. 6. Output spectrum from modulated measurement using a 20-MHz 10.5-dB-PAPR LTE signal centered at 3.6 GHz.

in Class-AB and Class-C modes, respectively. The large-signal frequency response of the fabricated circuit is measured using a network analyzer (Keysight N5230A PNA-L) with a driver amplifier in precedence to the DUT. The measured S21 at different power levels is presented in Fig. 4.

In the continuous-wave measurement, a power-swept single-tone signal is used to measure the Doherty PA performance within the pass-band. Fig. 5(a) shows the measured efficiency and gain at two in-band frequencies of 3.5 and 3.6 GHz. A peak efficiency of $> 60\%$ is measured together with an enhanced efficiency of $> 50\%$ at 6-dB output back-off (OBO) power level. A strong Doherty behavior is experimentally demonstrated. The CW measurement is extended to the entire pass-band from 3.4 to 3.8 GHz, as shown in Fig. 5(b). Peak output power of $40 - 42$ dBm, saturation efficiency of 55-

68%, and 6-dB OBO efficiency of 47-55% are measured. In Table I, the performance of this design is compared to the best recently reported works on the PA-filter integration. It can be seen that this design of integrated Doherty-filter engender significantly enhanced back-off efficiency with a comparable peak efficiency.

Moreover, a 20-MHz-bandwidth 64-QAM LTE signal with a PAPR of 10.5 dB is used for the modulated testing. The LTE signal is generated and analyzed with Keysight PXIe vector transceiver (VXT M9421). For an average output power of 33 dBm, the measured output spectrum and constellation diagram at 3.5 GHz are shown in Fig. 6. The ACLR of < -37 dB and EVM of 2.3% are measured without any digital predistortion, and the corresponding average efficiency is 47%.

V. Conclusion

This paper introduces the co-design of DPA and bandpass filter, in which the filter is designed as a post-matching network replacing the conventional quarter-wave transformer. As a result, the circuit complexity and inter-connection loss are minimized, which eventually enhances the overall performance. As a proof-of-concept demonstration, a linear and efficient GaN-based DPA is co-designed with a third-order 20%-FBW Hairpin filter at 3.6-GHz center frequency. Experimental results show not only the desired filter response but also the featured efficiency enhancement at power back-off. A state-of-the-art efficiency and linearity are achieved in the CW and LTE evaluation. Based upon the solid realistic validation, the co-design of Doherty-filter offers an effective solution for realizing highly compact and energy-efficient radio frontend, which are strongly demanded in 5G massive MIMO systems.

Acknowledgment

This work was supported in part by the National Science Foundation (NSF), Division Of Electrical, Communication and Cyber Systems (ECCS), under Award No. 1914875.

References

[1] K. Chen, J. Lee, W. J. Chappell, and D. Peroulis, "Co-design of highly efficient power amplifier and high-*q* output bandpass filter," *IEEE Transactions on Microwave Theory and Techniques*, vol. 61, no. 11, pp. 3940–3950, 2013.

[2] K. Chen, T. Lee, and D. Peroulis, "Co-design of multi-band high-efficiency power amplifier and three-pole high-*q* tunable filter," *IEEE Microwave and Wireless Components Letters*, vol. 23, no. 12, pp. 647–649, 2013.

[3] J. A. Estrada, P. de Paco, S. Johannes, D. Psychogiou, and Z. Popović, "Co-designed high-efficiency GaN filter power amplifier," in *2020 IEEE/MTT-S International Microwave Symposium (IMS)*, pp. 115–118, 2020.

[4] L. H. Zhou, X. Y. Zhou, W. S. Chan, J. Z. Pang, and D. Ho, "Integrated filtering Class-F power amplifier based on microstrip multimode resonator," in *2020 IEEE/MTT-S International Microwave Symposium (IMS)*, pp. 119–122, 2020.

[5] Y. C. Li, Q. Chen, Q. Xue, and J. Mou, "Filtering power amplifier with wide bandwidth using discriminating coupling," *IEEE Transactions on Circuits and Systems I: Regular Papers*, vol. 66, no. 10, pp. 3822–3830, 2019.

[6] S. Y. Zheng, Z. W. Liu, Y. M. Pan, Y. Wu, W. S. Chan, and Y. Liu, "Bandpass filtering Doherty power amplifier with enhanced efficiency and wideband harmonic suppression," *IEEE Transactions on Circuits and Systems I: Regular Papers*, vol. 63, no. 3, pp. 337–346, 2016.

[7] J. Wang, S. He, F. You, W. Shi, J. Peng, and C. Li, "Codesign of high-efficiency power amplifier and ring-resonator filter based on a series of continuous modes and even–odd-mode analysis," *IEEE Transactions on Microwave Theory and Techniques*, vol. 66, no. 6, pp. 2867–2878, 2018.

[8] J. Pang, S. He, C. Huang, Z. Dai, J. Peng, and F. You, "A post-matching doherty power amplifier employing low-order impedance inverters for broadband applications," *IEEE Transactions on Microwave Theory and Techniques*, vol. 63, no. 12, pp. 4061–4071, 2015.

[9] Z. Yang, Y. Yao, M. Li, Y. Jin, T. Li, Z. Dai, F. Tang, and Z. Li, "Bandwidth extension of doherty power amplifier using complex combining load with noninfinity peaking impedance," *IEEE Transactions on Microwave Theory and Techniques*, vol. 67, no. 2, pp. 765–777, 2019.

[10] K. Chen, E. J. Naglich, Y.-C. Wu, and D. Peroulis, "Highly linear and highly efficient dual-carrier power amplifier based on low-loss rf carrier combiner," *IEEE Transactions on Microwave Theory and Techniques*, vol. 62, no. 3, pp. 590–599, 2014.

[11] L. Zhou, X. Y. Zhou, W. S. Chan, T. Sharma, and D. Ho, "Wideband Class-F^{-1} power amplifier with dual-/quad-mode bandpass response," *IEEE Transactions on Circuits and Systems I: Regular Papers*, vol. 67, no. 7, pp. 2239–2249, 2020.

[12] Q.-Y. Guo, X. Y. Zhang, J.-X. Xu, Y. C. Li, and Q. Xue, "Bandpass class-f power amplifier based on multifunction hybrid cavity–microstrip filter," *IEEE Transactions on Circuits and Systems II: Express Briefs*, vol. 64, no. 7, pp. 742–746, 2017.